

METAL ABUNDANCES IN EXTREMELY DISTANT GALACTIC OLD OPEN CLUSTERS. II. BERKELEY 22 AND BERKELEY 66¹

SANDRO VILLANOVA

Dipartimento di Astronomia, Università di Padova, Vicolo Osservatorio 5, I-35122 Padua, Italy; villanova@pd.astro.it

GIOVANNI CARRARO^{2,3}

Departamento de Astronomía, Universidad de Chile, Casilla 36-D, Santiago de Chile, Chile; gcarraro@das.uchile.cl

FABIO BRESOLIN

Institute for Astronomy, 2680 Woodlawn Drive, Honolulu, HI 96822; bresolin@ifa.hawaii.edu

AND

FERDINANDO PATAT

ESO, Karl-Schwarzschild-Strasse 2, 85748 Garching, Germany; fpatat@eso.org

Received 2005 March 7; accepted 2005 April 12

ABSTRACT

We report on high-resolution spectroscopy of four giant stars in the Galactic old open clusters Berkeley 22 and Berkeley 66 obtained with HIRES at the Keck telescope. We find that $[\text{Fe}/\text{H}] = -0.32 \pm 0.19$ and -0.48 ± 0.24 for Be 22 and Be 66, respectively. Based on these data, we first revise the fundamental parameters of the clusters and then discuss them in the context of the Galactic disk radial abundance gradient. We found that both clusters nicely obey the most updated estimate of the slope of the gradient from the work of Friel and coworkers and are genuine Galactic disk objects.

Key words: open clusters and associations: general — open clusters and associations:
individual (Berkeley 22, Berkeley 66)

Online material: machine-readable table

1. INTRODUCTION

This paper is the second of a series dedicated to obtaining high-resolution spectroscopy of distant Galactic old open cluster giant stars to derive new or improved estimates of their metal content. In Carraro et al. (2004, hereafter Paper I) we presented results for Be 29 and Saurer 1, the two old open clusters possessing the largest galactocentric distance known, and showed that they do not belong to the disk but to the Monoceros feature (see also the discussion in Frinchaboy et al. [2005]). Here we present high-resolution spectra of four giant stars in the old open clusters Be 22 and Be 66. The latter cluster is of particular interest, since its heliocentric distance is among the largest currently known.

With this paper we aim to enlarge the sample of old open clusters with metallicity obtained from high-resolution spectra and to test the common assumption of axisymmetry made in chemical evolution models about the structure of the Milky Way disk. For this purpose we selected two open clusters of about the same age, one (Be 66) located in the second Galactic quadrant and the other (Be 22) in the third Galactic quadrant. Significant differences in metal abundance for clusters located in different disk zones will hopefully provide useful clues about

the chemical evolution of the disk and about the role of accretion and infall phenomena.

The layout of the paper is as follows: §§ 2 and 3 illustrate the observations and the data reduction strategies, while § 4 deals with radial velocity determinations. In § 5 we derive the stellar abundances, and in § 6 we revise the cluster fundamental parameters. The radial abundance gradient and the abundance ratios are discussed in §§ 7 and 8, respectively. The results of this paper are finally discussed in § 9.

2. OBSERVATIONS

The observations were carried out on the night of 2004 November 30 at the W. M. Keck Observatory under photometric conditions and a typical seeing of 1". The HIRES spectrograph (Vogt et al. 1994) on the Keck I telescope was used with a 1"1 × 7" slit to provide a spectral resolution $R = 34,000$ in the wavelength range 5200–8900 Å on the three 2048 × 4096 CCDs of the mosaic detector. A blocking filter was used to remove second-order contamination from blue wavelengths. Three exposures of 1500–1800 s were obtained for the stars Be 22-400 and Be 22-579. For both Be 66-785 and Be 66-934, we took four exposures of 2700 s each. During the first part of the night, when the telescope pointed to Be 66, the observing conditions were far from optimal because of the presence of thick clouds. For this reason, our abundance analysis in this first cluster is limited to Be 66-785. For the wavelength calibration, spectra of a thorium-argon lamp were secured after the set of exposures for each star was completed. The radial velocity standard HD 82106 was observed at the end of the night.

In Figure 1 we show a finding chart for the two clusters where the four observed stars are indicated, while in Figure 2 we show

¹ The data presented herein were obtained at the W. M. Keck Observatory, which is operated as a scientific partnership among the California Institute of Technology, the University of California, and the National Aeronautics and Space Administration. The Observatory was made possible by the generous financial support of the W. M. Keck Foundation.

² Dipartimento di Astronomia, Università di Padova, Vicolo Osservatorio 5, I-35122 Padua, Italy.

³ Astronomy Department, Yale University, New Haven, CT 06520-8101.

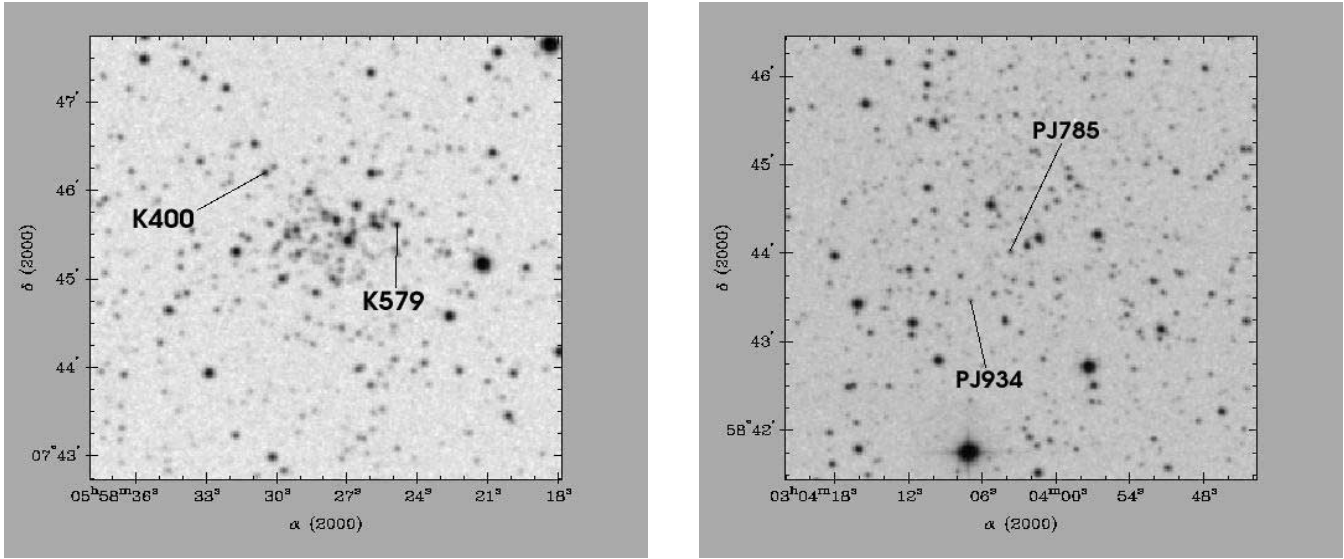


FIG. 1.—Digital Sky Survey finding charts of the observed stars in Be 22 (*left*) and Be 66 (*right*).

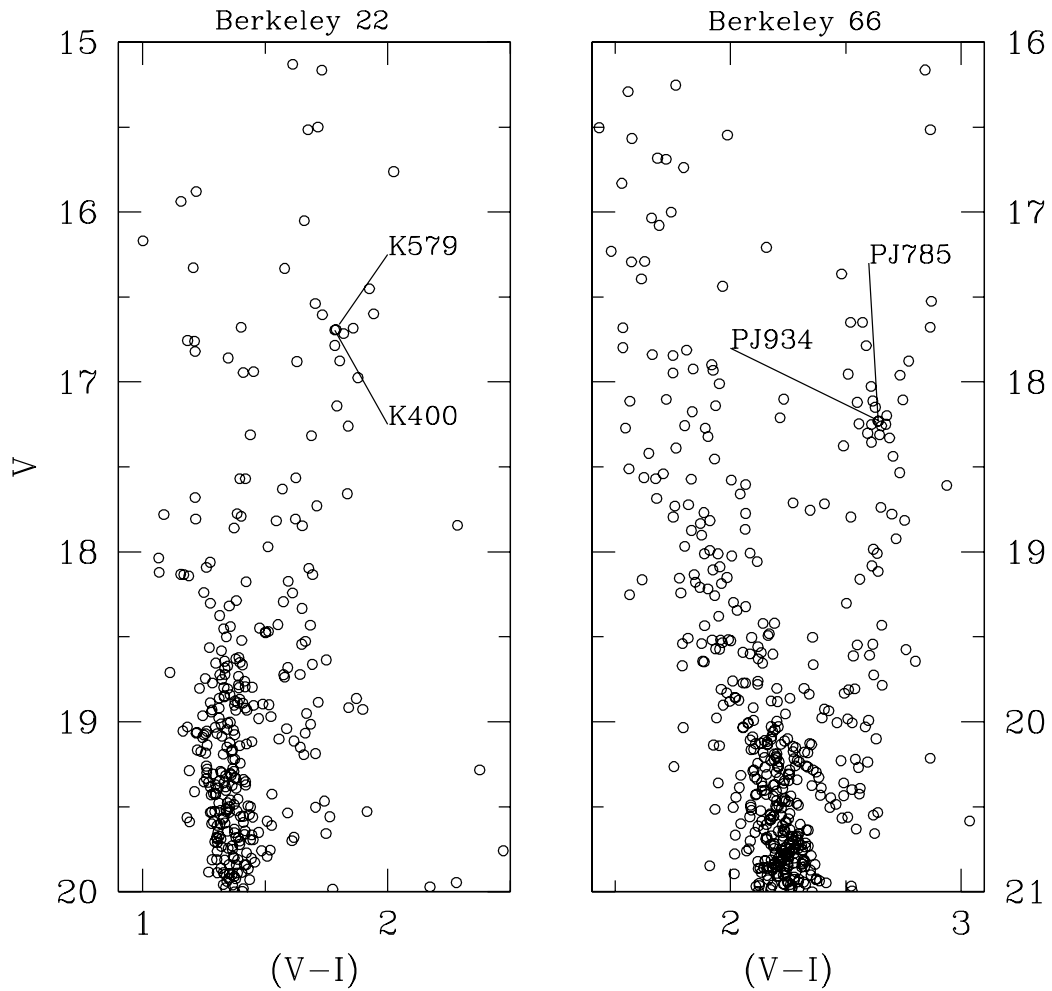


FIG. 2.—Position of the observed stars in the CMD of Be 22 (*left*; photometry from Kaluzny [1994]) and Be 66 (*right*; photometry from Phelps & Janes [1996]).

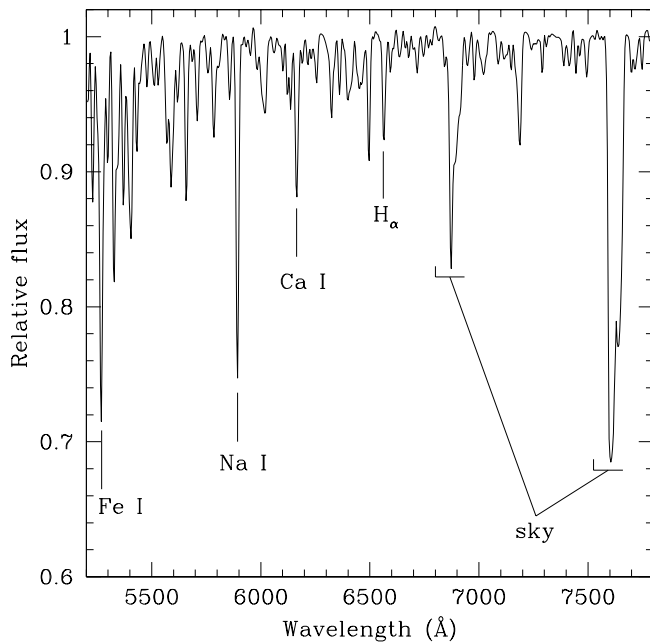


FIG. 3.—Example of an extracted spectrum for the star Be 22-400, with the main lines indicated.

the position of the stars in the color-magnitude diagram (CMD), based on published photometry (Kaluzny 1994; Phelps & Janes 1996).

3. DATA REDUCTION

Images were reduced using IRAF,⁴ including bias subtraction, flat-field correction, frame combination, extraction of spectral orders, wavelength calibration, sky subtraction, and spectral rectification. The single orders were merged into a single spectrum. As an example, we show in Figure 3 a portion of the reduced, normalized spectrum of Be 22-400.

4. RADIAL VELOCITIES

No radial velocity estimates were previously available for Be 22 or Be 66. The radial velocities of the target stars were measured using the IRAF *fxcor* task, which cross-correlates the object spectrum with the template (HD 82106). The peak of the cross-correlation was fitted with a Gaussian curve after rejecting the spectral regions contaminated by telluric lines ($\lambda > 6850$ Å). In order to check our wavelength calibration, we also measured the radial velocity of HD 82106 itself, by cross-correlation with a solar spectrum template. We obtained a radial heliocentric

⁴ IRAF is distributed by the National Optical Astronomy Observatory, which is operated by the Association of Universities for Research in Astronomy, Inc., under cooperative agreement with the National Science Foundation.

TABLE 1
OBSERVED STARS

ID	R.A.	Decl.	V	$(B - V)$	$(V - I)$	V_{rad} (km s ⁻¹)	S/N	Spectral Type	Comments
Be 22-400	05 58 30.97	+07 46 15.3	16.70	1.58	1.78	93.3 ± 0.2	25	G8 III	Kaluzny (1994)
Be 22-579	05 58 25.78	+07 45 31.2	16.88	1.66	1.80	97.3 ± 0.2	20	K0 III	Kaluzny (1994)
Be 66-785	03 04 02.90	+58 43 57.0	18.23	...	2.64	-50.7 ± 0.1	15	K1 III	Phelps & Janes (1996)
Be 66-934	03 04 06.41	+58 43 31.0	18.23	...	2.64	-50.6 ± 0.3	5	K1 III	Phelps & Janes (1996)

NOTE.—Units of right ascension are hours, minutes, and seconds, and units of declination are degrees, arcminutes, and arcseconds.

TABLE 2
ADOPTED ATMOSPHERIC PARAMETERS

ID	T_{eff} (K)	$\log(g)$ (dex)	v_t (km s ⁻¹)
Be 22-400	4790 ± 100	2.8 ± 0.1	1.3
Be 22-579	4690 ± 50	2.8 ± 0.1	1.2
Be 66-785	4640 ± 100	2.7 ± 0.1	1.2
Be 66-934

velocity of 29.8 ± 0.1 km s⁻¹, which perfectly matches the published value (29.7 km s⁻¹; Udry et al. 1999). The final error in the radial velocities was typically about 0.2 km s⁻¹. The two stars we measured in each cluster have compatible radial velocities (see Table 1) and are therefore considered bona fide cluster members.

5. ABUNDANCE ANALYSIS

5.1. Atomic Parameters and Equivalent Widths

We derived equivalent widths of spectral lines by using the standard IRAF routine *splot*. Repeated measurements show a typical error of about 5–10 mÅ for the weakest lines. The line list (Fe I, Fe II, Mg, Si, Ca, Al, Na, Ni, and Ti; see Table 3) was taken from Friel et al. (2003), who considered only lines with equivalent widths narrower than 150 mÅ in order to avoid non-linear effects in the LTE analysis of the spectral features. The $\log(gf)$ parameters of these lines were redetermined using equivalent widths from the solar spectrum template, solar abundances from Anders & Grevesse (1989), and standard solar parameters [$T_{\text{eff}} = 5777$ K, $\log(g) = 4.44$, and $v_t = 0.8$ km s⁻¹].

5.2. Atmospheric Parameters

Initial estimates of the atmospheric parameter T_{eff} were obtained from photometric observations in the optical. *BVI* data were available for Be 22 (Kaluzny 1994), while *VI* photometry for Be 66 was taken from Phelps & Janes (1996). Reddening values are $E(B - V) = 0.62$ [$E(V - I) = 0.74$] and $E(V - I) = 1.60$, respectively. First, estimated effective temperatures were derived from the $(V - I)$ - T_{eff} and $(B - V)$ - T_{eff} relations, the former from Alonso et al. (1999) and the latter from Gratton et al. (1996). We then adjusted the effective temperature by minimizing the slope of the abundances obtained from Fe I lines with respect to the excitation potential in the curve of growth analysis. For both clusters, the derived temperature yields a reddening consistent with the photometric one.

Initial guesses for the gravity $\log(g)$ were derived from

$$\log\left(\frac{g}{g_{\odot}}\right) = \log\left(\frac{M}{M_{\odot}}\right) + 4 \log\left(\frac{T_{\text{eff}}}{T_{\odot}}\right) - \log\left(\frac{L}{L_{\odot}}\right), \quad (1)$$

TABLE 3
EQUIVALENT WIDTHS

Element	λ (Å)	Excitation Potential	$\log(gf)$	Be 22-400	Be 22-579	Be 66-785
Fe I.....	5379.570	3.680	-1.57	83	102	...
Fe I.....	5417.033	4.415	-1.45	45	44	54
Fe I.....	5466.988	3.573	-2.24	69
Fe I.....	5633.946	4.990	-0.23	68	86	...
Fe I.....	5662.520	4.160	-0.59	106	111	...
Fe I.....	5701.550	2.560	-2.19	125	113	146
Fe I.....	5753.120	4.240	-0.76	102	108	94
Fe I.....	5775.081	4.220	-1.17	96	77	82
Fe I.....	5809.218	3.883	-1.67	80	83	...
Fe I.....	6024.058	4.548	+0.03	124	108	104
Fe I.....	6034.036	4.310	-2.35	58
Fe I.....	6056.005	4.733	-0.48	84	82	71
Fe I.....	6082.72	2.22	-3.62	77	76	...
Fe I.....	6093.645	4.607	-1.38	47
Fe I.....	6096.666	3.984	-1.82	47	46	...
Fe I.....	6151.620	2.180	-3.34	63	103	81
Fe I.....	6165.360	4.143	-1.53	47	66	...
Fe I.....	6173.340	2.220	-2.90	115	101	104
Fe I.....	6200.313	2.608	-2.38	124	102	81
Fe I.....	6229.230	2.845	-2.93	82
Fe I.....	6246.320	3.590	-0.77	119
Fe I.....	6344.15	2.43	-2.90	116	107	78
Fe I.....	6481.880	2.280	-2.95	121	109	97
Fe I.....	6574.229	0.990	-5.11	97	92	90
Fe I.....	6609.120	2.560	-2.67	108	93	125
Fe I.....	6703.570	2.758	-3.08	78	71	52
Fe I.....	6705.103	4.607	-1.07	57	60	...
Fe I.....	6733.151	4.638	-1.48	37
Fe I.....	6810.263	4.607	-0.99	64	72	...
Fe I.....	6820.372	4.638	-1.14	50	56	...
Fe I.....	6839.831	2.559	-3.42	70	67	74
Fe I.....	7540.430	2.730	-3.87	56
Fe I.....	7568.900	4.280	-0.85	80	92	91
Fe II.....	5414.080	3.22	-3.60	27
Fe II.....	6084.100	3.20	-3.78	21
Fe II.....	6149.250	3.89	-2.67	36
Fe II.....	6247.560	3.89	-2.31	63	48	...
Fe II.....	6369.463	2.89	-4.18	28
Fe II.....	6456.390	3.90	-2.05	50	57	...
Fe II.....	6516.080	2.89	-3.24	...	56	...
Fe I.....	6696.03	3.14	-1.56	71	...	43
Fe I.....	6698.67	3.13	44	...
Ca I.....	5581.97	2.52	-0.62	114	119	107
Ca I.....	5590.12	2.52	-0.82	105	112	100
Ca I.....	5867.57	2.93	-1.65	45
Ca I.....	6161.30	2.52	-1.27	93	109	92
Ca I.....	6166.44	2.52	-1.12	94	83	103
Ca I.....	6455.60	2.52	-1.41	82	70	72
Ca I.....	6499.65	2.52	-0.91	117	111	85
Mg I.....	5711.09	4.33	-1.71	117	109	...
Mg I.....	7387.70	5.75	-1.09	105	67	...
Na I.....	5682.65	2.10	-0.75	126	128	...
Na I.....	5688.21	2.10	-0.72	136	138	160
Na I.....	6154.23	2.10	-1.61	56	45	51
Na I.....	6160.75	2.10	-1.38	73	73	64
Ni I.....	6175.37	4.09	-0.52	74	64	62
Ni I.....	6176.81	4.09	-0.19	116	78	80
Ni I.....	6177.25	1.83	-3.60	36	42	...
Ni I.....	6223.99	4.10	64
Si I.....	5665.60	4.90	-1.98	...	53	...
Si I.....	5684.52	4.93	-1.63	56
Si I.....	5701.12	4.93	-1.99	...	41	...
Si I.....	5793.08	4.93	-1.89	38	49	...
Si I.....	6142.49	5.62	-1.47	27

TABLE 3—Continued

Element	λ (Å)	Excitation Potential	$\log(gf)$	Be 22-400	Be 22-579	Be 66-785
Si I.....	6145.02	5.61
Si I.....	6243.82	5.61	-1.30	39	54	...
Si I.....	7034.91	5.87	-0.74	55	103	...
Ti I.....	5978.54	1.87	-0.65	71	67	67
Ti II.....	5418.77	1.58	-2.12	74	76	103

NOTE.—Table 3 is also available in machine-readable form in the electronic edition of the *Astronomical Journal*.

taken from Carretta & Gratton (1997). In this equation, the mass M/M_{\odot} was derived from the comparison between the position of the star in the Hertzsprung-Russell diagram and the Padova isochrones (Girardi et al. 2000). The luminosity L/L_{\odot} was derived from the absolute magnitude M_V , assuming the literature distance moduli of 15.9 for Be 22 (Kaluzny 1994) and 17.4 for Be 66 (Phelps & Janes 1996). The bolometric correction (BC) was derived from the BC- T_{eff} relation from Alonso et al. (1999). The input $\log(g)$ values were then adjusted in order to satisfy the ionization equilibrium of Fe I and Fe II during the abundance analysis. Finally, the microturbulence velocity is given by the relation (Gratton et al. 1996)

$$v_t (\text{km s}^{-1}) = (1.19 \times 10^{-3}) T_{\text{eff}} - 0.90 \log(g) - 2. \quad (2)$$

The final adopted parameters are listed in Table 2.

5.3. Abundance Determination

The LTE abundance program MOOG (freely distributed by C. Sneden, University of Texas, Austin) was used to determine the metal abundances. Model atmospheres were interpolated from the grid of Kurucz (1992) models by using the values of T_{eff} and $\log(g)$ determined as explained in § 5.2. During the abundance analysis T_{eff} , $\log(g)$, and v_t were adjusted to remove trends in excitation potential, ionization equilibrium, and equivalent width for Fe I and Fe II lines. Table 3 contains the atomic parameters and equivalent widths for the lines used. The first column contains the name of the element, the second the wavelength in angstroms, the third the excitation potential, the fourth the oscillator strength $\log(gf)$, and the remaining columns the equivalent widths of the lines for the observed stars.

The derived abundances are listed in Table 4, together with their uncertainties. The measured iron abundances are $[\text{Fe}/\text{H}] = -0.32 \pm 0.19$ and -0.48 ± 0.24 for Be 22 and Be 66, respectively. The reported errors are derived from the uncertainties on the single-star abundance determination (see Table 4). For Be 66-934, no abundance determination was possible because the signal-to-noise ratio (S/N) in our spectrum was too low to perform any equivalent width determination.

Finally, using the stellar parameters [colors, T_{eff} , and $\log(g)$] and the absolute calibration of the MK system (Straizys &

Kuriliene 1981), we derived the stellar spectral classification, which we provide in Table 1.

6. REVISION OF CLUSTER PROPERTIES

Our study is the first to provide spectral abundance determinations of stars in Be 22 and Be 66. Here we briefly discuss the revision of the properties of these two clusters, which follow from our measured chemical abundances (see Figs. 4 and 5). We use the isochrone fitting method and adopt for this purpose the Padova models from Girardi et al. (2000).

6.1. Berkeley 22

Be 22 is an old open cluster located in the third Galactic quadrant, first studied by Kaluzny (1994). On the basis of deep *VI* photometry, he derived an age of 3 Gyr, a distance of 6.0 Kpc, and a reddening $E(V - I) = 0.74$. The author suggests that the probable metal content of the cluster is lower than solar. Here we obtained $[\text{Fe}/\text{H}] = -0.32$, which corresponds to $Z = 0.008$ and roughly half the solar metal content. Very recently, Di Fabrizio et al. (2005) presented new *BVI* photometry, on the basis of which they derived a younger age (2.0–2.5 Gyr) but similar reddening and distance, also suggesting that the cluster possesses solar metal abundance. The two photometric studies are compatible in the *VI* filters, with the difference in the *V* and *I* zero points being less than 0.03 mag. Both the studies show that the cluster turnoff is located at $V = 19$ and that a clump is at $V = 16.65$.

According to Carraro & Chiosi (1994), with $\Delta V \approx 2.35$ mag (ΔV being the magnitude difference between the turnoff and the clump) and for the derived metallicity, one would expect an age around 3.5 Gyr. This preliminary estimate of the age is in fact confirmed by the isochrone fitting method. In Figure 4 the solid line is a 3.3 Gyr isochrone, which provides a new age estimate of 3.3 ± 0.3 Gyr for the same photometric reddening and galactocentric distance derived by Kaluzny (1994). Both the turnoff and the clump location are nicely reproduced. The uncertainty reflects the range of isochrones that produce an acceptable fit.

For comparison, in the same figure we superpose a solar-metallicity isochrone for the age of 2.25 Gyr (Fig. 4, *dashed line*) and for the same reddening and distance reported by Di Fabrizio et al. (2005). This isochrone clearly does not provide a comparable good fit. When trying to fit the turnoff, both

TABLE 4
MEAN STELLAR ABUNDANCES

ID	[Fe I/H]	[Fe II/H]	[Al I/H]	[Ca I/H]	[Mg I/H]	[Na I/H]	[Ni I/H]	[Si I/H]	[Ti/H]
Be 22-400.....	-0.29 ± 0.21	-0.32 ± 0.19	+0.05 ± 0.20	-0.35 ± 0.11	-0.37 ± 0.20	-0.23 ± 0.05	-0.26 ± 0.20	-0.37 ± 0.08	-0.19 ± 0.11
Be 22-579.....	-0.35 ± 0.17	-0.28 ± 0.04	-0.12 ± 0.20	-0.45 ± 0.11	-0.41 ± 0.14	-0.33 ± 0.12	-0.29 ± 0.07	-0.20 ± 0.11	-0.22 ± 0.04
Be 66-785.....	-0.48 ± 0.24	...	-0.48 ± 0.20	-0.53 ± 0.21	...	-0.33 ± 0.18	-0.24 ± 0.25	...	-0.05 ± 0.23

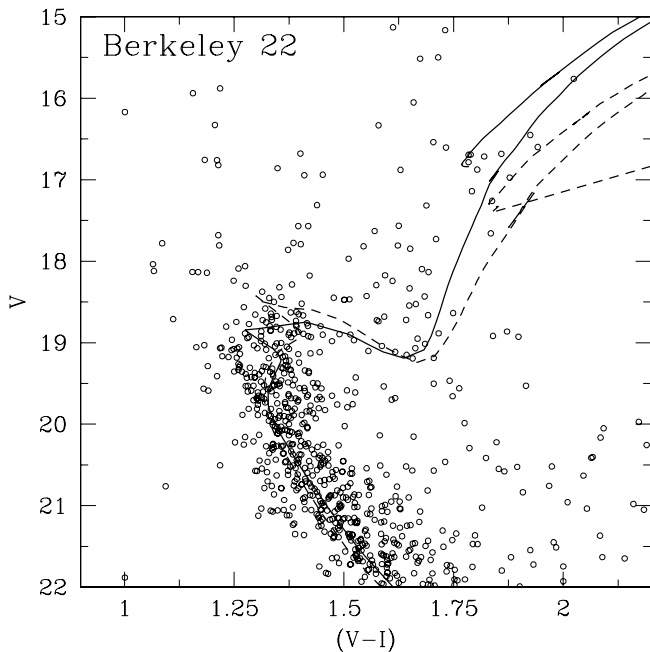


FIG. 4.—Isochrone solution for Be 22 (photometry from Kaluzny [1994]). The solid line is a 3.3 Gyr isochrone for $Z = 0.008$, while the dashed one is a 2.25 Gyr isochrone for $Z = 0.019$. See text for details.

the color of the red giant branch and the position of the clump cannot be reproduced.

6.2. Berkeley 66

Be 66 was studied by Guarneri & Carraro (1997) and Phelps & Janes (1996), who suggested a reddening $E(V - I) = 1.60$ and a metallicity in the range $-0.23 \leq [\text{Fe}/\text{H}] \leq 0.0$. By assuming these values, Phelps & Janes (1996) derived a galactocentric distance of 12.9 kpc and an age of 3.5 Gyr. We obtain a

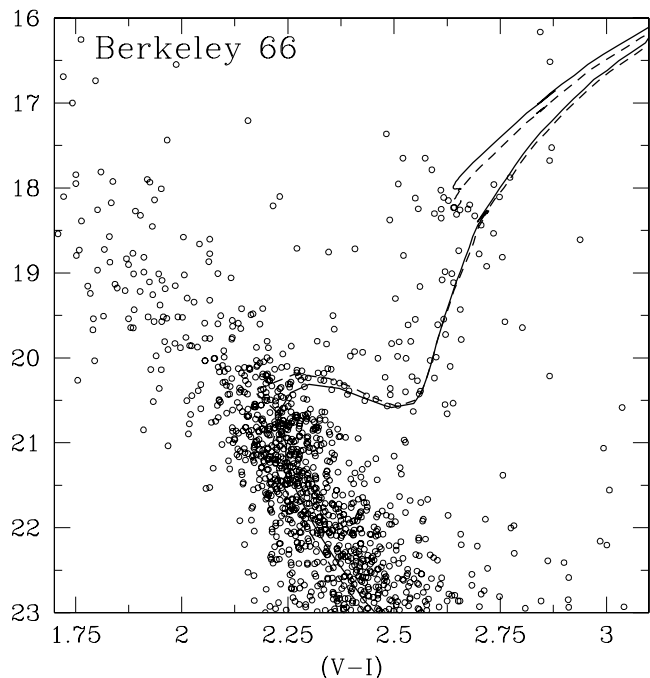


FIG. 5.—Isochrone solution for Be 66 (photometry from Phelps & Janes [1996]). The solid and dashed lines are two $Z = 0.008$ isochrones, for the age of 5 and 4 Gyr, respectively. See text for details.

significantly smaller abundance value, $[\text{Fe}/\text{H}] = -0.48 \pm 0.24$, for a spectroscopic reddening of $E(V - I) = 1.60$, which is consistent with the Phelps & Janes (1996) estimate. By looking at the CMD, the turnoff is situated at $V = 20.75$, whereas the clump is at $V = 18.25$, implying a ΔV of 2.5. For this ΔV and the derived $[\text{Fe}/\text{H}]$, the Carraro & Chiosi (1994) calibration yields an age of about 4.7 Gyr, significantly larger than the previous estimate. The value $[\text{Fe}/\text{H}] = -0.48$ translates into $Z = 0.006$, and we generated a few isochrones for this exact metal abundance from Girardi et al. (2000). The result is shown in Figure 5, where 4 and 5 Gyr isochrones (dashed and solid line, respectively) are superposed on the cluster CMD. Both the isochrones reasonably reproduce the turnoff shape, but the 5 Gyr one (solid line) clearly presents a clump that is too bright. On the other hand, the 4 Gyr isochrone reproduces well all the CMD features. This new age estimate provides a reddening $E(V - I) = 1.60$ and a heliocentric distance of 5 kpc.

7. THE RADIAL ABUNDANCE GRADIENT

In Figure 6 we plot the open cluster Galactic radial abundance gradient, as derived from Friel et al. (2002), which is at present the most updated version of the gradient itself. The clusters included in their work (squares) define an overall slope of -0.06 ± 0.01 dex kpc^{-1} (solid line). The circles represent the two clusters analyzed here, and it can be seen that they clearly follow the general trend very nicely. In fact, the dashed line, which represents the radial abundance gradient determined by including Be 22 and Be 66, basically coincides with that of Friel et al. (2002).

We note that the gradient exhibits quite a significant scatter. One may wonder whether this solely depends on observational errors, or whether this scatter reflects a true chemical inhomogeneity in the Galactic disk.

It must be noted, however, that between 10 and 14 kpc the scatter increases and the distribution of the cluster abundances is also compatible with a flat gradient. Again, it is extremely difficult to conclude whether this behavior of the gradient is significant, or whether the distribution of abundances is mostly

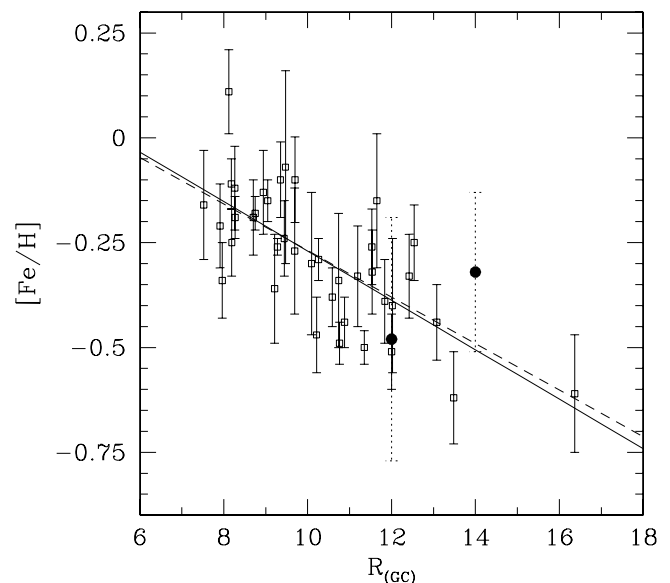


FIG. 6.—Galactic disk chemical abundance radial gradient. Squares are data from Friel et al. (2002), whereas the circles represent Be 22 and Be 66 (this work). The solid line is the linear fit to the Friel et al. (2002) data, whereas the dashed line is a linear fit to all the data points.

TABLE 5
ABUNDANCE RATIOS

ID	[Fe/H]	[Ca/Fe]	[Mg/Fe]	[Si/Fe]	[Ti/Fe]	[Na/Fe]	[Al/Fe]	[Ni/Fe]
Be 22-400	-0.29	-0.06	-0.08	-0.08	+0.10	+0.06	+0.34	+0.03
Be 22-579	-0.35	-0.10	-0.06	+0.15	+0.13	+0.02	+0.23	+0.06
Be 66-785	-0.48	-0.05	+0.43	+0.15	+0.00	+0.24

affected by the size of the observational errors and the small number of clusters involved.

8. ABUNDANCE RATIOS

Abundance ratios constitute a powerful tool for assigning clusters to stellar populations (Friel et al. 2003). In Paper I we found that Saurer 1 and Be 29 exhibit enhanced abundance ratios with respect to the Sun, and we concluded that they probably do not belong to the Galactic disk, since all the old open clusters for which detailed abundance analysis is available show solar-scale abundance ratios.

In Table 5 we list the abundance ratios for the observed stars in Be 22 and Be 66. Our program clusters have ages around 3–4 Gyr and iron metal content $[\text{Fe}/\text{H}] \approx -0.3$ – -0.4 . They are therefore easily comparable with similar clusters from the literature, such as Tombaugh 2 and Melotte 66 (see Friel et al. 2003, Table 7). We note that the latter two clusters and our program clusters have scaled solar abundances. Indeed, at a similar $[\text{Fe}/\text{H}]$ and age, Be 22 and Melotte 66 have similar values for all the abundance ratios.

Similar conclusions can be drawn for Be 66 when compared with Tombaugh 2, an old open cluster of similar age and $[\text{Fe}/\text{H}]$. All the abundance ratios we could measure are comparable in these two clusters. These results therefore indicate that Be 22 and Be 66 are two genuine old disk clusters that fit well in the overall Galactic radial abundance gradient (see § 7).

9. DISCUSSION AND CONCLUSIONS

Be 22 and Be 66 are two similar age open clusters located at roughly symmetric positions with respect to the virtual line

connecting the Sun to the Galactic center. In fact, for Be 22 we derive +5.5, -2.0, and -0.8 kpc for the rectangular Galactic coordinates X , Y , and Z , respectively, while for Be 66 we obtain +4, +2.5, and 0.01 kpc. The corresponding galactocentric distances R_{GC} are 12.7 and 14.2 kpc for Be 66 and Be 22, respectively.

Within the errors, the two clusters possess the same metal abundance, suggesting that at the distance of 12–14 kpc from the Galactic center the metal distribution over the second and third quadrant of the Galaxy is basically the same.

It is worthwhile to point out here that only three clusters are thus far known to lie outside the 14 kpc radius ring from the Galactic center: Be 20, Be 29, and Saurer 1. Paper I showed that both Be 29 and Saurer 1 do not belong to the disk, and therefore we are probably sampling here the real outskirts of the Galactic stellar disk.

The axisymmetric homogeneity is confirmed when we add a few more old open clusters located in this strip, such as NGC 1193, NGC 2158, NGC 2141, Be 31, Tombaugh 2, and Be 21 (Friel et al. 2002). All these clusters are located in the second and third quadrant, have metallicities $-0.62 < [\text{Fe}/\text{H}] < -0.25$, and probably all belong to the same generation (ages between 2 and 4 Gyr). Therefore, we conclude that at 12–14 kpc the disk is chemically homogeneous in $[\text{Fe}/\text{H}]$ within the observational errors, although with a significant spread. The scatter, if real, may be due to local inhomogeneities.

The work of G. C. is supported by Fundación Andes. We thank the anonymous referee for his/her report, which helped a lot to improve the paper presentation.

REFERENCES

- Alonso, A., Arribas, S., & Martínez-Roger, C. 1999, *A&AS*, 140, 261
 Anders, E., & Grevesse, N. 1989, *Geochim. Cosmochim. Acta*, 53, 197
 Carraro, G., Bresolin, F., Villanova, S., Matteucci, F., Patat, F., & Romaniello, M. 2004, *AJ*, 128, 1676 (Paper I)
 Carraro, G., & Chiosi, C. 1994, *A&A*, 287, 761
 Carretta, E., & Gratton, R. G. 1997, *A&AS*, 121, 95
 Di Fabrizio, L., Bragaglia, A., Tosi, M., & Marconi, G. 2005, *MNRAS*, 359, 966
 Friel, E. D., Jacobson, H. R., Barrett, E., Fullton, L., Balachandran, A. C., & Pilachowski, C. A. 2003, *AJ*, 126, 2372
 Friel, E. D., Janes, K. A., Tavares, M., Jennifer, S., Katsanis, R., Lotz, J., Hong, L., & Miller, N. 2002, *AJ*, 124, 2693
 Frinchauboy, P. M., Munoz, R. R., Majewski, S. R., Friel, E. D., Phelps, R. L., & Kunkel, W. B. 2005, in *Chemical Abundances and Mixing in Stars in the Milky Way Galaxy and its Satellites*, ed. L. Pasquini & S. Randich (Berlin: Springer), in press (astro-ph/0411127)
 Girardi, L., Bressan, A., Bertelli, G., & Chiosi, C. 2000, *A&AS*, 141, 371
 Gratton, R. G., Carretta, E., & Castelli, F. 1996, *A&A*, 314, 191
 Guarnieri, D., & Carraro, G. 1997, *A&AS*, 121, 451
 Kaluzny, J. 1994, *A&AS*, 108, 151
 Kurucz, R. L. 1992, in *IAU Symp. 149, The Stellar Populations of Galaxies*, ed. B. Barbuy & A. Renzini (Dordrecht: Kluwer), 225
 Phelps, R. L., & Janes, K. A. 1996, *AJ*, 111, 1604
 Straizys, V., & Kuriliene, G. 1981, *Ap&SS*, 80, 353
 Udry, S., Mayor, M., & Queloz, D. 1999, in *IAU Colloq. 170., Precise Stellar Radial Velocities*, ed. J. B. Hearnshaw & C. D. Scarfe (ASP Conf. Ser. 185; San Francisco: ASP), 367
 Vogt, S. S., et al. 1994, *Proc. SPIE*, 2198, 362